



Crystal structure and Hirshfeld surface analysis of ethyl 2-[5-(3-chlorobenzyl)-6-oxo-3-phenyl-1,6-dihydropyridazin-1-yl]acetate

Fouad El Kalai,^{a*} Cemile Baydere,^{b*} Said Daoui,^a Rafik Saddik,^c Necmi Dege,^b Khalid Karrouchi^d and Nouredine Benchat^a

Received 24 April 2019

Accepted 21 May 2019

Edited by M. Weil, Vienna University of Technology, Austria

Keywords: crystal structure; pyridazine; Hirshfeld surface analysis.

CCDC reference: 1917654

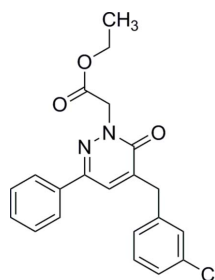
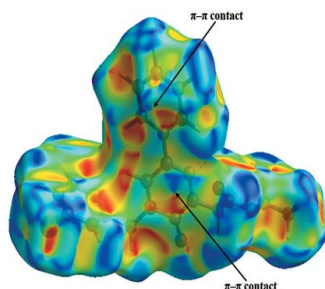
Supporting information: this article has supporting information at journals.iucr.org/e

^aLaboratory of Applied Chemistry and Environment (LCAE), Faculty of Sciences, Mohamed I University, 60000 Oujda, Morocco, ^bDepartment of Physics, Faculty of Arts and Sciences, Ondokuz Mayıs University, 55139-Samsun, Turkey, ^cLaboratory Organic synthesis, Extraction and Valorization, Faculty of Sciences, Ain Chok, University Hassan II, Casablanca, Morocco, and ^dLaboratory of Plant Chemistry, Organic and Bioorganic Synthesis, URAC23, Faculty of Science, BP 1014, GEOPAC Research Center, Mohammed V University, Rabat, Morocco. *Correspondence e-mail: fouadelkalai80@gmail.com, cemle28baydere@hotmail.com

The title pyridazinone derivative, C₂₁H₁₉ClN₂O₃, is not planar. The unsubstituted phenyl ring and the pyridazine ring are inclined to each other, making a dihedral angle of 17.41 (13)^o whereas the Cl-substituted phenyl ring is nearly orthogonal to the pyridazine ring [88.19 (13)^o]. In the crystal, C—H...O hydrogen bonds generate dimers with R₂²(10) and R₂²(24) ring motifs which are linked by C—H...O interactions, forming chains extending parallel to the *c*-axis direction. The intermolecular interactions were investigated using Hirshfeld surface analysis and two-dimensional fingerprint plots, revealing that the most significant contributions to the crystal packing are from H...H (44.5%), C...H/H...C (18.5%), H...O/H...O (15.6%), Cl...H/H...Cl (10.6%) and C...C (2.8%) contacts.

1. Chemical context

Pyridazines are an important family of six-membered aromatic heterocycles (Akhtar *et al.*, 2016). The related compound pyridazinone is an important pharmacophore with a wide range of biological applications (Asif, 2015), and its chemistry has been studied for several decades. Pyridazinones are used as scaffolds for potential drug candidates (Dubey & Bhosle, 2015; Thakur *et al.*, 2010) because of their significant potential as antimicrobial (Sönmez *et al.*, 2006), antidepressant (Boukharsa *et al.*, 2016), anti-inflammatory (Barberot *et al.*, 2018), antihypertensive (Siddiqui *et al.*, 2011), analgesic (Gökçe *et al.*, 2009), anti-HIV (Livermore *et al.*, 1993), anti-convulsant (Partap *et al.*, 2018; Sharma *et al.*, 2014), cardio-tonic (Wang *et al.*, 2008), antihistaminic (Tao *et al.*, 2012), glucan synthase inhibitors (Zhou *et al.*, 2011), phosphodiesterase (PDE) inhibitors (Ochiai *et al.*, 2012) and herbicidal (Asif, 2013) agents.



OPEN ACCESS

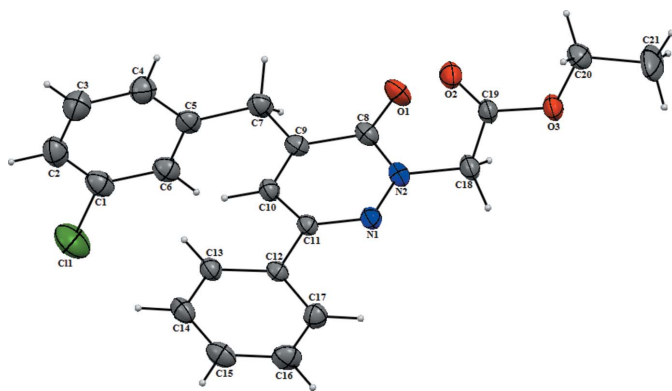


Figure 1
The molecular structure of the title compound with displacement ellipsoids drawn at the 50% probability level.

In this context and in a continuation of our work in this field (Chkirate *et al.*, 2019a,b; Karrassi *et al.*, 2015, 2016a,b), we report herein the synthesis and the molecular and crystal structures of the title pyridazinone derivative, together with its Hirshfeld surface analysis.

2. Structural commentary

The molecule of the title compound is not planar (Fig. 1). The unsubstituted phenyl ring (C12–C17) and the pyridazine ring (C8–C11/N1/N2) are twisted relative to each other, making a dihedral angle of 17.41 (13)°; the chloro-substituted phenyl ring (C1–C6) is inclined to the pyridazine ring by 88.19 (13)°. Atoms C8 and N2 of the pyridazine ring show the largest deviations from planarity (root-mean-square deviation = 0.0236 Å) in positive and negative directions [C8 = 0.0357 (15) Å; N2 = –0.0319 (14) Å]. The O1=C8 bond length of the pyridazinone carbonyl function is 1.230 (3) Å, and the N1–N2 bond length in the pyridazine ring is 1.362 (2) Å, both in accordance with values for related pyridazinones.

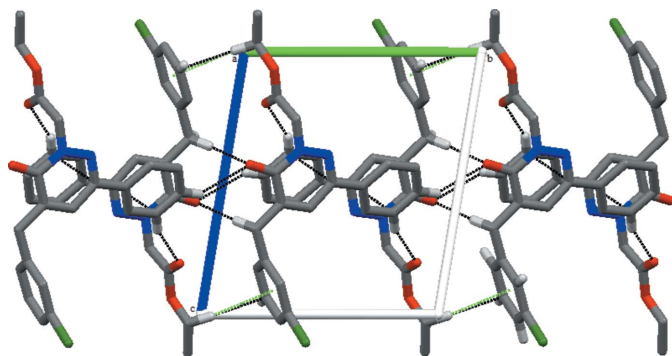


Figure 2
A view along the *a* axis of the crystal structure of the title compound. Black dashed lines symbolize intermolecular C–H...O hydrogen bonds; C–H... π interactions are shown as green dashed lines.

Table 1
Hydrogen-bond geometry (Å, °).

Cg2 is the centroid of the C1–C6 phenyl ring

<i>D</i> –H... <i>A</i>	<i>D</i> –H	H... <i>A</i>	<i>D</i> ... <i>A</i>	<i>D</i> –H... <i>A</i>
C14–H14...O2 ⁱ	0.93	2.53	3.416 (3)	160
C7–H7B...O1 ⁱⁱ	0.97	2.54	3.485 (3)	164
C15–H15...O1 ⁱⁱⁱ	0.93	2.66	3.474 (3)	147
C20–H20B...Cg2 ^{iv}	0.97	2.81	3.759 (3)	165

Symmetry codes: (i) $-x, -y + 1, -z + 1$; (ii) $-x + 1, -y + 2, -z + 1$; (iii) $x - 1, y - 1, z$; (iv) $-x + 1, -y, -z + 1$.

3. Supramolecular features

The crystal packing exhibits C–H...O hydrogen bonds between aryl or methylene groups and carbonyl O atoms (Table 1), as well as C–H... π interactions and van der Waals contacts. Intermolecular C7–H7B...O1 and C14–H14...O2 hydrogen bonds produce $R_2^2(10)$ and $R_2^2(24)$ motif rings (Fig. 2), supplemented by C15–H15...O1 contacts, forming chains extending parallel to the *c* axis (Fig. 2). A weak C20–H20B...Cg2 ($-x + 1, -y, -z + 1$; Cg2 is the centroid of the C1–C6 phenyl ring) contact is also present in this chain (Table 1; Fig. 2). Weak aromatic π – π stacking interactions between adjacent pyridazine rings [Cg1...Cg1 ($-x + 1, -y + 1, -z + 1$) = 3.8833 (13) Å, where Cg1 is the centroid of the C8–C11/N1/N2 ring] along the *a* axis lead to the formation of a three-dimensional network.

4. Database survey

A search of the Cambridge Structural Database (CSD, version 5.40, update November 2018; Groom *et al.*, 2016) revealed two structures containing a similar pyridazinone moiety as in the title structure but with different substituents, *viz.* 4-benzyl-6-*p*-tolylpyridazin-3(2*H*)-one (YOTVIN; Oubair *et al.*, 2009) and ethyl 3-methyl-6-oxo-5-(3-(trifluoromethyl)phenyl)-1,6-dihydro-1-pyridazineacetate (QANVOR; Xu *et al.*, 2005). In the crystal structure of YOTVIN, the molecules are connected two-by-two through N–H...O hydrogen bonds with an $R_2^2(8)$ graph-set motif, forming dimers arranged around an inversion center. Weak C–H...O hydrogen bonds and weak offset π – π stacking stabilize the packing. In the crystal structure of QANVOR, the phenyl and pyridazinone rings are approximately co-planar, making a dihedral angle of 4.84 (13)°. Centrosymmetrically related molecules form dimers through non-classical intermolecular C–H...O hydrogen bonds.

5. Hirshfeld surface analysis

A Hirshfeld surface analysis (Spackman & Jayatilaka, 2009) and the associated two-dimensional fingerprint plots (McKinnon *et al.*, 2007) were performed with *Crystal-Explorer17* (Turner *et al.*, 2017), using a standard (high) surface resolution with the three-dimensional d_{norm} surfaces plotted over a fixed colour scale of –0.1647 (red) to 1.1730 (blue) a.u. The three-dimensional d_{norm} surface of the title

molecule is illustrated in Fig. 3a. The pale-red spots symbolize short contacts and negative d_{norm} values on the surface and correspond to the C—H...O interactions (Table 1).

The shape-index map of the title molecule was generated in the range -1 to 1 Å (Fig. 3b). The convex blue regions symbolize hydrogen-donor groups and the concave red regions hydrogen-acceptor groups. π - π interactions are generally indicated by adjacent red and blue triangles in the shape-index map, as is the case for the title molecule.

The curvedness map of the title complex was generated in the range -4.0 to 0.4 Å (Fig. 3c). The curvedness plot of the title complex shows large regions of green with a relatively flat (*i.e.* planar) surface area, indicating the presence of π - π stacking interactions, while the blue regions demonstrate areas of curvature.

The overall two-dimensional fingerprint plot is illustrated in Fig. 4a, delineated into H...H, H...C/C...H, H...O/O...H, H...Cl/Cl...H, C...C contacts associated with their relative contributions to the Hirshfeld surface in Fig. 4b–f, respectively. The most important intermolecular interaction is H...H, contributing 44.5% to the overall crystal packing, with the centre of the peak $d_e = d_i = 1.18$ Å (Fig. 4b). H...C/C...H contacts, with a 18.5% contribution to the Hirshfeld surface, indicate the presence of the weak C—H... π interaction (Table 1). Two pairs of characteristic wings in the fingerprint plot with pairs of tips at $d_e + d_i \sim 2.8$ Å are present (Fig. 4c). H...O/O...H contacts arising from intermolecular C—H...O hydrogen bonding make a 15.6% contribution to the Hirshfeld surface and are represented by a pair of sharp spikes in the region $d_e + d_i \sim 2.35$ Å. The C...C contacts are a measure of π - π stacking interactions and contribute 2.8% of the Hirshfeld surface. They appear as an arrow-shaped distribution at $d_e + d_i \sim 3.3$ Å. Another contact to the Hirshfeld surface is from H...Cl/Cl...H interactions (10.6%).

6. Synthesis and crystallization

To a solution (0.99 g, 3 mmol) of 4-(3-dichlorobenzyl)-6-phenylpyridazin-3(2H)-one in 30 ml of tetrahydrofuran (THF), potassium carbonate (0.5 g, 3.5 mmol) was added. The mixture was refluxed for 1 h. After cooling, ethyl bromoacetate (0.66 g, 4 mmol) was added and the mixture was refluxed for 8 h. The precipitated material was removed by

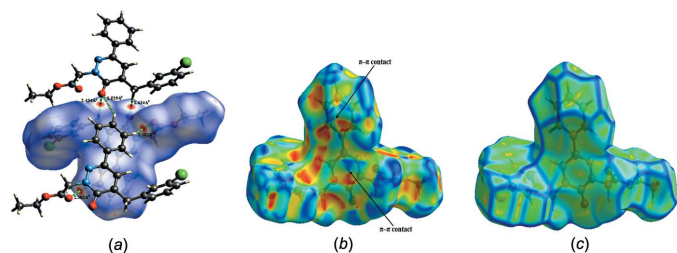


Figure 3
(a) d_{norm} mapped on the Hirshfeld surface for visualizing the intermolecular interactions, (b) shape-index map of the title compound and (c) curvedness map of the title compound.

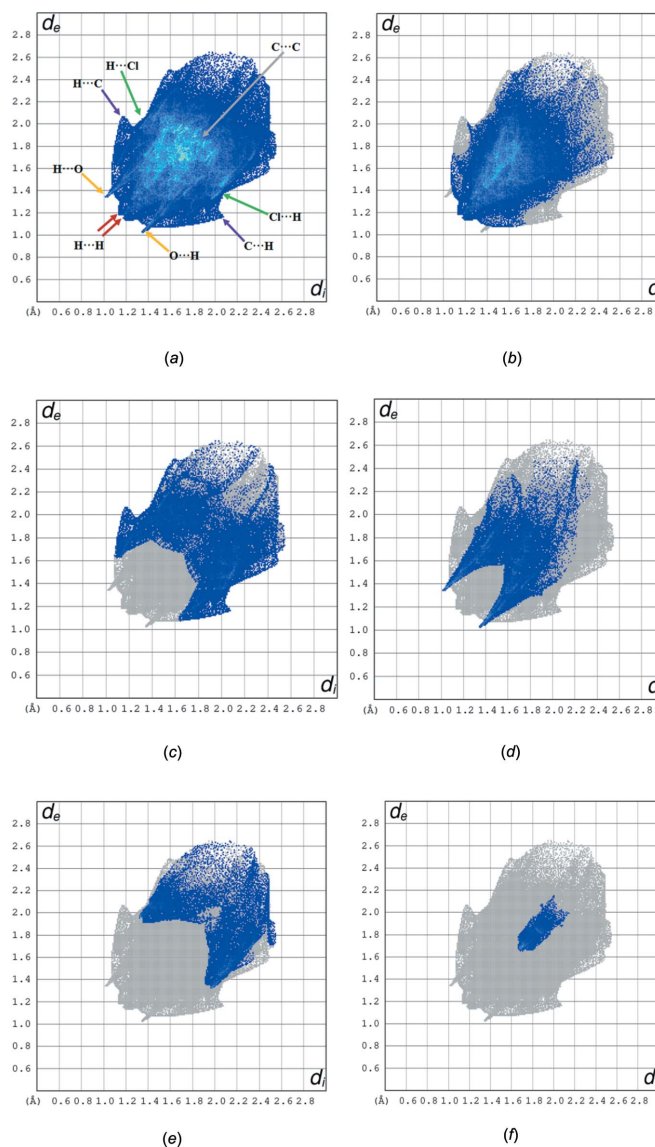


Figure 4
(a) The overall two-dimensional fingerprint plot, and delineated into (b) H...H, (c) H...C/C...H, (d) H...O/O...H, (e) H...Cl/Cl...H and (f) C...C interactions.

filtration and the solvent evaporated under vacuum. The residue was purified through silica gel column chromatography using hexane/ethyl acetate (4:6 *v/v*). Slow evaporation at room temperature led to formation of single crystals with a yield of 70%.

7. Refinement

Crystal data, data collection and structure refinement details are summarized in Table 2. Hydrogen atoms were fixed geometrically and treated as riding, with C—H = 0.97 Å for methyl [$U_{\text{iso}}(\text{H}) = 1.2U_{\text{eq}}(\text{C})$], C—H = 0.96 Å for methylene [$U_{\text{iso}}(\text{H}) = 1.5U_{\text{eq}}(\text{C})$], C—H = 0.93 Å for aromatic [$U_{\text{iso}}(\text{H}) = 1.2U_{\text{eq}}(\text{C})$] and C—H = 0.98 Å for methine [$U_{\text{iso}}(\text{H}) = 1.2U_{\text{eq}}(\text{C})$] H atoms.

Table 2

Experimental details.

Crystal data	
Chemical formula	C ₂₁ H ₁₉ ClN ₂ O ₃
<i>M_r</i>	382.83
Crystal system, space group	Triclinic, P $\bar{1}$
Temperature (K)	296
<i>a</i> , <i>b</i> , <i>c</i> (Å)	8.8410 (11), 10.3043 (12), 11.3610 (12)
α , β , γ (°)	94.801 (9), 103.596 (9), 106.905 (9)
<i>V</i> (Å ³)	949.6 (2)
<i>Z</i>	2
Radiation type	Mo <i>K</i> α
μ (mm ⁻¹)	0.23
Crystal size (mm)	0.88 × 0.53 × 0.19
Data collection	
Diffractometer	Stoe IPDS 2
Absorption correction	Integration (<i>X-RED32</i> ; Stoe & Cie, 2002)
<i>T_{min}</i> , <i>T_{max}</i>	0.876, 0.960
No. of measured, independent and observed [<i>I</i> > 2 σ (<i>I</i>)] reflections	9612, 3716, 2058
<i>R_{int}</i>	0.031
($\sin \theta/\lambda$) _{max} (Å ⁻¹)	0.617
Refinement	
<i>R</i> [<i>F</i> ² > 2 σ (<i>F</i> ²)], <i>wR</i> (<i>F</i> ²), <i>S</i>	0.047, 0.127, 0.91
No. of reflections	3716
No. of parameters	245
H-atom treatment	H-atom parameters constrained
$\Delta\rho_{\max}$, $\Delta\rho_{\min}$ (e Å ⁻³)	0.26, -0.34

Computer programs: *X-AREA* and *X-RED* (Stoe & Cie, 2002), *SHELXT2017* (Sheldrick, 2015a), *SHELXL2018* (Sheldrick, 2015b), *Mercury* (Macrae *et al.*, 2008), *WinGX* (Farrugia, 2012), *PLATON* (Spek, 2009) and *publCIF* (Westrip, 2010).

Acknowledgements

The authors acknowledge the Faculty of Arts and Sciences, Ondokuz Mayıs University, Turkey, for the use of the Stoe IPDS 2 diffractometer (purchased under grant F.279 of the University Research Fund).

References

Akhtar, W., Shaquiquzzaman, M., Akhter, M., Verma, G., Khan, M. F. & Alam, M. M. (2016). *Eur. J. Med. Chem.* **123**, 256–281.
 Asif, M. (2013). *Mini-Rev. Org. Chem.* **10**, 113–122.
 Asif, M. (2015). *Mini Rev. Med. Chem.* **14**, 1093–1103.
 Barberot, C., Moniot, A., Allart-Simon, I., Malleret, L., Yegorova, T., Laronze-Cochard, M., Bentaher, A., Médebielle, M., Bouillon, J. P., Hénon, E., Sapi, J., Velard, F. & Gérard, S. (2018). *Eur. J. Med. Chem.* **146**, 139–146.
 Boukharsa, Y., Meddah, B., Tiendrebeogo, R. Y., Ibrahim, A., Taoufik, J., Cherrah, Y., Benomar, A., Faouzi, M. E. A. & Ansar, M. (2016). *Med. Chem. Res.* **25**, 494–500.
 Chkirate, K., Kansiz, S., Karrouchi, K., Mague, J. T., Dege, N. & Essassi, E. M. (2019a). *Acta Cryst. E75*, 154–158.
 Chkirate, K., Kansiz, S., Karrouchi, K., Mague, J. T., Dege, N. & Essassi, E. M. (2019b). *Acta Cryst. E75*, 33–37.

Dubey, S. & Bhosle, P. A. (2015). *Med. Chem. Res.* **24**, 3579–3598.
 Farrugia, L. J. (2012). *J. Appl. Cryst.* **45**, 849–854.
 Gökçe, M., Utku, S. & Küpeli, E. (2009). *Eur. J. Med. Chem.* **44**, 3760–3764.
 Groom, C. R., Bruno, I. J., Lightfoot, M. P. & Ward, S. C. (2016). *Acta Cryst. B72*, 171–179.
 Karrouchi, K., Ansar, M., Radi, S., Saadi, M. & El Ammari, L. (2015). *Acta Cryst. E71*, o890–o891.
 Karrouchi, K., Radi, S., Ansar, M. H., Taoufik, J., Ghabbour, H. A. & Mabkhot, Y. N. (2016a). *Z. Kristallogr. New Cryst. Struct.* **231**, 883–886.
 Karrouchi, K., Radi, S., Ansar, M. H., Taoufik, J., Ghabbour, H. A. & Mabkhot, Y. N. (2016b). *Z. Kristallogr. New Cryst. Struct.* **231**, 839–841.
 Livermore, D., Bethell, R. C., Cammack, N., Hancock, A. P., Hann, M. M., Green, D., Lamont, R. B., Noble, S. A., Orr, D. C. & Payne, J. J. (1993). *J. Med. Chem.* **36**, 3784–3794.
 Macrae, C. F., Bruno, I. J., Chisholm, J. A., Edgington, P. R., McCabe, P., Pidcock, E., Rodriguez-Monge, L., Taylor, R., van de Streek, J. & Wood, P. A. (2008). *J. Appl. Cryst.* **41**, 466–470.
 McKinnon, J. J., Jayatilaka, D. & Spackman, M. A. (2007). *Chem. Commun.* pp. 3814–3816.
 Ochiai, K., Takita, S., Eiraku, T., Kojima, A., Iwase, K., Kishi, T., Fukuchi, K., Yasue, T., Adams, D. R., Allcock, R. W., Jiang, Z. & Kohno, Y. (2012). *Bioorg. Med. Chem.* **20**, 1644–1658.
 Oubair, A., Daran, J.-C., Fihri, R., Majidi, L. & Azrour, M. (2009). *Acta Cryst. E65*, o1350–o1351.
 Partap, S., Akhtar, M. J., Yar, M. S., Hassan, M. Z. & Siddiqui, A. A. (2018). *Bioorg. Chem.* **77**, 74–83.
 Sharma, B., Verma, A., Sharma, U. K. & Prajapati, S. (2014). *Med. Chem. Res.* **23**, 146–157.
 Sheldrick, G. M. (2015a). *Acta Cryst. A71*, 3–8.
 Sheldrick, G. M. (2015b). *Acta Cryst. C71*, 3–8.
 Siddiqui, A. A., Mishra, R., Shaharyar, M., Husain, A., Rashid, M. & Pal, P. (2011). *Bioorg. Med. Chem. Lett.* **21**, 1023–1026.
 Sönmez, M., Berber, I. & Akbaş, E. (2006). *Eur. J. Med. Chem.* **41**, 101–105.
 Spackman, M. A. & Jayatilaka, D. (2009). *CrystEngComm*, **11**, 19–32.
 Spek, A. L. (2009). *Acta Cryst. D65*, 148–155.
 Stoe & Cie (2002). *X-AREA* and *X-RED32*. Stoe & Cie GmbH, Darmstadt, Germany.
 Tao, M., Aimone, L. D., Gruner, J. A., Mathiasen, J. R., Huang, Z., Lyons, J., Raddatz, R. & Hudkins, R. L. (2012). *Bioorg. Med. Chem. Lett.* **22**, 1073–1077.
 Thakur, A. S., Verma, P. & Chandy, A. (2010). *Asian. J. Res. Chem.* **3**, 265–271.
 Turner, M. J., McKinnon, J. J., Wolff, S. K., Grimwood, D. J., Spackman, P. R., Jayatilaka, D. & Spackman, M. A. (2017). *CrystalExplorer17*. University of Western Australia. <http://hirshfeldsurface.net>.
 Wang, T., Dong, Y., Wang, L.-C., Xiang, B.-R., Chen, Z. & Qu, L.-B. (2008). *Arzneimittelforschung*, **58**, 569–573.
 Westrip, S. P. (2010). *J. Appl. Cryst.* **43**, 920–925.
 Xu, H., Song, H.-B., Yao, C.-S., Zhu, Y.-Q., Hu, F.-Z., Zou, X.-M. & Yang, H.-Z. (2005). *Acta Cryst. E61*, o1561–o1563.
 Zhou, G., Ting, P. C., Aslanian, R., Cao, J., Kim, D. W., Kuang, R., Lee, J. F., Schwerdt, J., Wu, H., Jason Herr, R., Zych, A. J., Yang, J., Lam, S., Wainhaus, S., Black, T. A., McNicholas, P. M., Xu, Y. & Walker, S. S. (2011). *Bioorg. Med. Chem. Lett.* **21**, 2890–2893.

supporting information

Acta Cryst. (2019). E75, 892-895 [https://doi.org/10.1107/S2056989019007424]

Crystal structure and Hirshfeld surface analysis of ethyl 2-[5-(3-chlorobenzyl)-6-oxo-3-phenyl-1,6-dihydropyridazin-1-yl]acetate

Fouad El Kalai, Cemile Baydere, Said Daoui, Rafik Saddik, Necmi Dege, Khalid Karrouchi and Nouredine Benchat

Computing details

Data collection: *X-AREA* (Stoe & Cie, 2002); cell refinement: *X-AREA* (Stoe & Cie, 2002); data reduction: *X-RED* (Stoe & Cie, 2002); program(s) used to solve structure: *SHELXT2017* (Sheldrick, 2015a); program(s) used to refine structure: *SHELXL2018* (Sheldrick, 2015b); molecular graphics: *Mercury* (Macrae *et al.*, 2008) and *PLATON* (Spek, 2009); software used to prepare material for publication: *WinGX* (Farrugia, 2012), *SHELXL2018* (Sheldrick, 2015b), *PLATON* (Spek, 2009) and *publCIF* (Westrip, 2010).

Ethyl 2-[5-(3-chlorobenzyl)-6-oxo-3-phenyl-1,6-dihydropyridazin-1-yl]acetate

Crystal data

$C_{21}H_{19}ClN_2O_3$

$M_r = 382.83$

Triclinic, $P\bar{1}$

$a = 8.8410$ (11) Å

$b = 10.3043$ (12) Å

$c = 11.3610$ (12) Å

$\alpha = 94.801$ (9)°

$\beta = 103.596$ (9)°

$\gamma = 106.905$ (9)°

$V = 949.6$ (2) Å³

$Z = 2$

$F(000) = 400$

$D_x = 1.339$ Mg m⁻³

Mo $K\alpha$ radiation, $\lambda = 0.71073$ Å

Cell parameters from 11025 reflections

$\theta = 3.0\text{--}31.4^\circ$

$\mu = 0.23$ mm⁻¹

$T = 296$ K

Prism, yellow

$0.88 \times 0.53 \times 0.19$ mm

Data collection

Stoe IPDS 2

diffractometer

Detector resolution: 6.67 pixels mm⁻¹

rotation method scans

Absorption correction: integration

(*X-RED32*; Stoe & Cie, 2002)

$T_{\min} = 0.876$, $T_{\max} = 0.960$

9612 measured reflections

3716 independent reflections

2058 reflections with $I > 2\sigma(I)$

$R_{\text{int}} = 0.031$

$\theta_{\max} = 26.0^\circ$, $\theta_{\min} = 3.0^\circ$

$h = -10 \rightarrow 10$

$k = -12 \rightarrow 12$

$l = -14 \rightarrow 14$

Refinement

Refinement on F^2

Least-squares matrix: full

$R[F^2 > 2\sigma(F^2)] = 0.047$

$wR(F^2) = 0.127$

$S = 0.91$

3716 reflections

245 parameters

0 restraints

Hydrogen site location: inferred from neighbouring sites

H-atom parameters constrained

$$w = 1/[\sigma^2(F_o^2) + (0.0666P)^2]$$

where $P = (F_o^2 + 2F_c^2)/3$
 $(\Delta/\sigma)_{\max} < 0.001$

$$\Delta\rho_{\max} = 0.26 \text{ e } \text{\AA}^{-3}$$

$$\Delta\rho_{\min} = -0.34 \text{ e } \text{\AA}^{-3}$$

Special details

Geometry. All esds (except the esd in the dihedral angle between two l.s. planes) are estimated using the full covariance matrix. The cell esds are taken into account individually in the estimation of esds in distances, angles and torsion angles; correlations between esds in cell parameters are only used when they are defined by crystal symmetry. An approximate (isotropic) treatment of cell esds is used for estimating esds involving l.s. planes.

Fractional atomic coordinates and isotropic or equivalent isotropic displacement parameters (\AA^2)

	x	y	z	$U_{\text{iso}}^*/U_{\text{eq}}$
Cl1	0.29831 (14)	0.53925 (11)	-0.10674 (8)	0.1264 (4)
O3	0.72303 (19)	0.86361 (16)	0.93869 (13)	0.0654 (5)
O2	0.4976 (2)	0.87323 (18)	0.80559 (15)	0.0704 (5)
O1	0.6649 (2)	0.89797 (17)	0.57180 (15)	0.0725 (5)
N1	0.4130 (2)	0.57611 (18)	0.60996 (15)	0.0503 (5)
N2	0.5368 (2)	0.69655 (18)	0.62523 (15)	0.0542 (5)
C12	0.1658 (3)	0.4089 (2)	0.49033 (17)	0.0463 (5)
C11	0.3033 (3)	0.5381 (2)	0.50375 (17)	0.0462 (5)
C19	0.6111 (3)	0.8315 (2)	0.83046 (19)	0.0536 (6)
C10	0.3151 (3)	0.6166 (2)	0.40745 (18)	0.0507 (5)
H10	0.238158	0.583782	0.331377	0.061*
C9	0.4352 (3)	0.7377 (2)	0.42376 (19)	0.0528 (6)
C13	0.0216 (3)	0.3784 (2)	0.39727 (19)	0.0556 (6)
H13	0.012681	0.437926	0.340794	0.067*
C8	0.5539 (3)	0.7869 (2)	0.5427 (2)	0.0557 (6)
C5	0.3334 (3)	0.7688 (2)	0.2046 (2)	0.0602 (6)
C17	0.1752 (3)	0.3177 (2)	0.5723 (2)	0.0617 (6)
H17	0.270130	0.335520	0.636054	0.074*
C18	0.6531 (3)	0.7357 (2)	0.7459 (2)	0.0618 (6)
H18A	0.762208	0.780076	0.737838	0.074*
H18B	0.654649	0.653680	0.781667	0.074*
C14	-0.1095 (3)	0.2608 (3)	0.3867 (2)	0.0659 (7)
H14	-0.206077	0.242734	0.324506	0.079*
C6	0.3669 (3)	0.6883 (3)	0.1175 (2)	0.0693 (7)
H6	0.465811	0.669538	0.134709	0.083*
C15	-0.0967 (4)	0.1717 (3)	0.4678 (3)	0.0735 (7)
H15	-0.183752	0.091911	0.460255	0.088*
C7	0.4550 (3)	0.8283 (2)	0.3280 (2)	0.0659 (7)
H7A	0.565102	0.846300	0.318471	0.079*
H7B	0.444144	0.915570	0.356666	0.079*
C20	0.6983 (3)	0.9534 (3)	1.0330 (2)	0.0697 (7)
H20A	0.592464	0.912468	1.048073	0.084*
H20B	0.702185	1.041629	1.007747	0.084*
C16	0.0439 (4)	0.1999 (3)	0.5596 (3)	0.0749 (8)
H16	0.051884	0.138934	0.614912	0.090*
C1	0.2528 (4)	0.6351 (3)	0.0037 (2)	0.0752 (8)

C4	0.1844 (4)	0.7928 (3)	0.1767 (2)	0.0752 (8)
H4	0.160060	0.847345	0.234301	0.090*
C2	0.1061 (4)	0.6593 (3)	-0.0218 (3)	0.0839 (9)
H2	0.030067	0.622809	-0.097796	0.101*
C3	0.0711 (4)	0.7371 (3)	0.0646 (3)	0.0902 (9)
H3	-0.029726	0.752677	0.047719	0.108*
C21	0.8330 (5)	0.9709 (4)	1.1455 (3)	0.1279 (16)
H21A	0.936252	1.019422	1.131745	0.192*
H21B	0.834403	0.882260	1.164831	0.192*
H21C	0.815587	1.022374	1.212596	0.192*

Atomic displacement parameters (Å²)

	U^{11}	U^{22}	U^{33}	U^{12}	U^{13}	U^{23}
Cl1	0.1545 (9)	0.1266 (8)	0.0925 (6)	0.0370 (7)	0.0468 (6)	-0.0221 (5)
O3	0.0619 (10)	0.0768 (11)	0.0468 (8)	0.0251 (9)	-0.0023 (8)	-0.0084 (7)
O2	0.0597 (11)	0.0818 (12)	0.0620 (10)	0.0286 (9)	0.0007 (8)	-0.0056 (8)
O1	0.0687 (11)	0.0536 (10)	0.0731 (11)	-0.0058 (9)	0.0156 (9)	-0.0070 (8)
N1	0.0517 (11)	0.0514 (11)	0.0437 (10)	0.0153 (9)	0.0090 (8)	0.0008 (8)
N2	0.0504 (11)	0.0545 (11)	0.0460 (10)	0.0091 (10)	0.0048 (8)	-0.0036 (8)
C12	0.0519 (13)	0.0456 (12)	0.0411 (11)	0.0144 (10)	0.0158 (10)	0.0004 (9)
C11	0.0502 (13)	0.0478 (12)	0.0386 (11)	0.0162 (11)	0.0100 (10)	0.0005 (9)
C19	0.0475 (13)	0.0558 (13)	0.0452 (12)	0.0093 (11)	0.0012 (10)	0.0008 (9)
C10	0.0563 (14)	0.0501 (13)	0.0401 (11)	0.0141 (11)	0.0086 (10)	0.0009 (9)
C9	0.0594 (14)	0.0458 (12)	0.0505 (12)	0.0126 (11)	0.0175 (11)	0.0015 (9)
C13	0.0589 (14)	0.0537 (13)	0.0475 (12)	0.0142 (12)	0.0098 (11)	-0.0004 (10)
C8	0.0573 (15)	0.0511 (13)	0.0525 (13)	0.0119 (12)	0.0145 (11)	-0.0035 (10)
C5	0.0752 (17)	0.0482 (13)	0.0541 (13)	0.0100 (12)	0.0218 (12)	0.0158 (10)
C17	0.0624 (16)	0.0636 (15)	0.0562 (13)	0.0174 (13)	0.0130 (12)	0.0126 (11)
C18	0.0541 (14)	0.0672 (15)	0.0505 (12)	0.0165 (12)	-0.0014 (11)	-0.0082 (11)
C14	0.0514 (15)	0.0637 (16)	0.0668 (15)	0.0067 (13)	0.0084 (12)	-0.0105 (13)
C6	0.0742 (18)	0.0634 (15)	0.0690 (16)	0.0162 (13)	0.0246 (14)	0.0100 (12)
C15	0.0699 (18)	0.0566 (16)	0.0838 (18)	0.0018 (13)	0.0295 (15)	-0.0022 (14)
C7	0.0793 (18)	0.0524 (14)	0.0592 (14)	0.0114 (12)	0.0179 (13)	0.0110 (11)
C20	0.0812 (19)	0.0734 (17)	0.0524 (13)	0.0277 (14)	0.0147 (13)	-0.0022 (12)
C16	0.091 (2)	0.0592 (16)	0.0750 (17)	0.0149 (16)	0.0318 (16)	0.0214 (13)
C1	0.095 (2)	0.0646 (16)	0.0622 (16)	0.0137 (16)	0.0299 (15)	0.0051 (12)
C4	0.089 (2)	0.0779 (18)	0.0639 (16)	0.0308 (16)	0.0244 (15)	0.0151 (13)
C2	0.092 (2)	0.085 (2)	0.0601 (16)	0.0142 (17)	0.0099 (16)	0.0108 (14)
C3	0.088 (2)	0.101 (2)	0.083 (2)	0.0356 (18)	0.0183 (17)	0.0193 (17)
C21	0.156 (3)	0.171 (4)	0.0489 (16)	0.091 (3)	-0.0186 (19)	-0.0337 (18)

Geometric parameters (Å, °)

Cl1—C1	1.724 (3)	C17—H17	0.9300
O3—C19	1.331 (2)	C18—H18A	0.9700
O3—C20	1.454 (3)	C18—H18B	0.9700
O2—C19	1.187 (3)	C14—C15	1.362 (4)

O1—C8	1.230 (3)	C14—H14	0.9300
N1—C11	1.304 (2)	C6—C1	1.391 (4)
N1—N2	1.362 (2)	C6—H6	0.9300
N2—C8	1.378 (3)	C15—C16	1.359 (4)
N2—C18	1.450 (3)	C15—H15	0.9300
C12—C17	1.383 (3)	C7—H7A	0.9700
C12—C13	1.385 (3)	C7—H7B	0.9700
C12—C11	1.487 (3)	C20—C21	1.484 (4)
C11—C10	1.420 (3)	C20—H20A	0.9700
C19—C18	1.502 (3)	C20—H20B	0.9700
C10—C9	1.347 (3)	C16—H16	0.9300
C10—H10	0.9300	C1—C2	1.360 (4)
C9—C8	1.447 (3)	C4—C3	1.378 (4)
C9—C7	1.500 (3)	C4—H4	0.9300
C13—C14	1.386 (3)	C2—C3	1.363 (4)
C13—H13	0.9300	C2—H2	0.9300
C5—C6	1.378 (3)	C3—H3	0.9300
C5—C4	1.380 (4)	C21—H21A	0.9600
C5—C7	1.503 (3)	C21—H21B	0.9600
C17—C16	1.384 (4)	C21—H21C	0.9600
C19—O3—C20	116.13 (18)	C13—C14—H14	120.1
C11—N1—N2	116.83 (18)	C5—C6—C1	120.0 (3)
N1—N2—C8	126.86 (17)	C5—C6—H6	120.0
N1—N2—C18	114.58 (19)	C1—C6—H6	120.0
C8—N2—C18	118.35 (19)	C16—C15—C14	119.7 (2)
C17—C12—C13	117.8 (2)	C16—C15—H15	120.1
C17—C12—C11	121.31 (19)	C14—C15—H15	120.1
C13—C12—C11	120.81 (19)	C9—C7—C5	114.18 (19)
N1—C11—C10	121.6 (2)	C9—C7—H7A	108.7
N1—C11—C12	116.04 (18)	C5—C7—H7A	108.7
C10—C11—C12	122.40 (17)	C9—C7—H7B	108.7
O2—C19—O3	125.0 (2)	C5—C7—H7B	108.7
O2—C19—C18	126.11 (19)	H7A—C7—H7B	107.6
O3—C19—C18	108.9 (2)	O3—C20—C21	106.6 (2)
C9—C10—C11	121.50 (19)	O3—C20—H20A	110.4
C9—C10—H10	119.3	C21—C20—H20A	110.4
C11—C10—H10	119.3	O3—C20—H20B	110.4
C10—C9—C8	118.4 (2)	C21—C20—H20B	110.4
C10—C9—C7	125.0 (2)	H20A—C20—H20B	108.6
C8—C9—C7	116.5 (2)	C15—C16—C17	121.1 (3)
C12—C13—C14	121.3 (2)	C15—C16—H16	119.4
C12—C13—H13	119.4	C17—C16—H16	119.4
C14—C13—H13	119.4	C2—C1—C6	120.6 (3)
O1—C8—N2	120.3 (2)	C2—C1—C11	119.6 (2)
O1—C8—C9	125.2 (2)	C6—C1—C11	119.8 (3)
N2—C8—C9	114.5 (2)	C3—C4—C5	120.9 (3)
C6—C5—C4	118.5 (2)	C3—C4—H4	119.6

C6—C5—C7	121.1 (3)	C5—C4—H4	119.6
C4—C5—C7	120.4 (2)	C1—C2—C3	119.7 (3)
C12—C17—C16	120.2 (2)	C1—C2—H2	120.1
C12—C17—H17	119.9	C3—C2—H2	120.1
C16—C17—H17	119.9	C2—C3—C4	120.3 (3)
N2—C18—C19	112.24 (19)	C2—C3—H3	119.9
N2—C18—H18A	109.2	C4—C3—H3	119.9
C19—C18—H18A	109.2	C20—C21—H21A	109.5
N2—C18—H18B	109.2	C20—C21—H21B	109.5
C19—C18—H18B	109.2	H21A—C21—H21B	109.5
H18A—C18—H18B	107.9	C20—C21—H21C	109.5
C15—C14—C13	119.8 (2)	H21A—C21—H21C	109.5
C15—C14—H14	120.1	H21B—C21—H21C	109.5

Hydrogen-bond geometry (Å, °)

Cg2 is the centroid of the C1–C6 phenyl ring

<i>D</i> —H... <i>A</i>	<i>D</i> —H	H... <i>A</i>	<i>D</i> ... <i>A</i>	<i>D</i> —H... <i>A</i>
C14—H14...O2 ⁱ	0.93	2.53	3.416 (3)	160
C7—H7B...O1 ⁱⁱ	0.97	2.54	3.485 (3)	164
C15—H15...O1 ⁱⁱⁱ	0.93	2.66	3.474 (3)	147
C20—H20B... <i>Cg2</i> ^{iv}	0.97	2.81	3.759 (3)	165

Symmetry codes: (i) $-x, -y+1, -z+1$; (ii) $-x+1, -y+2, -z+1$; (iii) $x-1, y-1, z$; (iv) $-x+1, -y, -z+1$.